Quantification of Relative Chromatin Content in Flow Cytometry Standards using 3D OPTM Imaging Technique

Nitin Agarwal[*a], Alberto M. Biancardi[b], Florence W. Patten[c], Anthony P. Reeves[b], Eric J. Seibel[d]

[a]Department of Bioengineering, University of Washington, Seattle, WA
[b]School of Electrical and Computer Engineering, Cornell University, Ithaca NY
[c]VisionGate Inc., Phoenix, AZ
[d]Department of Mechanical Engineering, University of Washington, Seattle, WA

ABSTRACT

A potential biomarker for early diagnosis of cancer is assessment of high nuclear DNA content. Conventional hematoxylin staining is neither stoichiometric nor reproducible. Although feulgen stain is stoichiometric, it is time consuming and destroys nuclear morphology. We used acidic thionin stain, which can be stoichiometric and also preserve the nuclear morphology used in conventional cytology. Fifty chicken erythrocyte nuclei singlets (CENs), diploid trout erythrocyte nuclei (TENs) and Triploid TENs were stained for 15 and 30 minutes each. After imaging with optical projection tomography microscope (OPTM), 3D reconstructions of the nuclei were processed to calculate chromatin content. The mean of ratios of individual observations was compared with standard ratios of DNA indices of the flow cytometry standards. Mean error, standard deviation and 97% confidence interval (CI) was computed for the ratios of these standards. At 15 and 30 minutes, the ratio of Triploid TEN to TEN was 1.72 and 1.76, TEN to CEN was 1.27 and 2.01 and Triploid TEN to CEN was 2.11 and 3.39 respectively. Estimates of DNA indices for all 3 types of nuclei had less mean error at 30 minutes of staining; Triploid TEN to TEN 0.349±0.04, TEN to CEN 0.36±0.04 and Triploid TEN to CEN 0.64 ± 0.07. In conclusion, imaging of cells with thionin staining at 30 minutes and 3D reconstruction provides quantitative assessment of cell chromatin content. The addition of this quantitative feature of aneuploidy is expected to add greater accuracy to a classifier for early diagnosis of cancer based on 3D cytological imaging.

Keywords: DNA content, chromatin, acidic thionin, optical microscopy, 3D reconstruction, quantitative cytology

1. INTRODUCTION

Cancer is the *leading* cause of death in economically developed countries and the *second leading* cause of death in developing countries. One of the common factors for the poor outcome in cancer is lack of accurate and efficient methods for early diagnosis. The conventional means for making a diagnosis is extracting isolated cells and having them examined by cytologists. Automated computer-aided analysis of slides has been used to automate the screening process[1,2,3]. However, cells and their nuclear chromatin features are three dimensional (3D) and hence analysis using slides, which are two dimensional (2D), will not give accurate results for cancer diagnosis. The ability to image sub-nuclear 3D structures using absorptive dyes was demonstrated by Fauver et al[4], who introduced the optical projection tomography microscope (OPTM). This instrument images cells and nuclei within a rotating capillary tube using a bright field optical microscope with focal plane scanning method. The OPTM combines attributes of optical CT (computed tomography) imaging with flow cytometry. Optical projections of the stained cell are obtained and 3D reconstructions are generated using algorithms similar to conventional X-ray CT. Cells and nuclei are flowed within the spinning capillary tube, so high throughput screening is possible. Recently, OPTM technique has been shown to increase the sensitivity and specificity of cancer diagnosis compared to conventional examination based on 2D slides[5].

In addition to 'site' and 'type' specific tests for cancer diagnosis, which are usually late, an important biomarker for early cytological diagnosis of any cancer is aneuploidy, an abnormally high DNA content[6]. However, conventional hematoxylin (H of H & E) stain is neither stoichiometric nor reproducible[7,8], so it cannot provide quantitative information about DNA content for early diagnosis. Feulgen stain though stoichiometric is time consuming and it also destroys the diagnostic morphology of the cell[7,9,10]. Thus, a stain, which is both stoichiometric and also

preserves the nuclear morphology, is likely to provide a better quantitative estimation of DNA content (aneuploidy measure). With this aim in mind, we chose acidic thionin stain, utilizing its stoichiometric staining property while preserving the nuclear morphology. Thionin is a basic stain, which binds to the DNA. It is also sometimes used as alternative to Schiff reagent in feulgen staining technique[11]. Other groups have measured aneuploidy based on Automated Cellular Imaging System (ACIS) (Chroma Vision Medical System Inc., San Juan Capistrano CA) which uses feulgen stain, along with a simple bright field microscope[12,13,14,15,16]. Later with the help of software, the nucleus is segmented out and its total intensity is calculated to give its aneuploidy measurement. However these results are inaccurate, as analysis has only been performed using 2D images.

In this study we have used, for the first time quantitative assessment of chromatin content with 3D OPTM images. It had been shown that 3D images of single cells provided by OPTM result in threefold reduction in false negative rate for adenocarcinoma detection as compared to 2D images with a similar high 96% specificity[5]. Hence, our quantitative assessment is expected to provide a far more accurate and robust results as compared to previous studies for cancer diagnosis.

Internal biological standards of known chromatin content are used as specimens for this study. These samples have a know DNA content relative to the total chromatin content of normal human diploid cells and are typically used for calibrating flow cytometers. By staining and imaging both unknown human cells mixed with these standards, the measure of total chromatin in human cells is less susceptible to variations in staining and measurement variability. In this preliminary study, three flow cytometry standards of bare nuclei are stained, imaged, and measured for chromatin content relative to one another. The DNA index, which is defined as the ratio of the mean DNA content of the G_o/G_1 sample peak divided by the mean DNA content of normal diploid G_o/G_1 human cell peak, are 0.35 (35%) for chicken erythrocyte nuclei singlets (CEN), 0.80 (80%) for diploid trout erythrocyte nuclei (TEN) and 1.2 (120%) for triploid trout erythrocyte nuclei (Triploid TEN). The overall goal is to add the new feature of aneuploidy measurement to the more conventional cytological measures of nuclear morphology in order to make a more powerful and robust classifier for early cancer diagnosis.

2. METHODS

With an aim of staining cells with different DNA content, we took CENs, TENs and Triploid TENs (Biosure, Inc. USA), which are used as internal standards to calibrate the flow cytometer. They have a DNA index of 35%, 80% and 120% relative to human diploid cells respectively.

2.1 FACS OF CONTROL STANDARDS

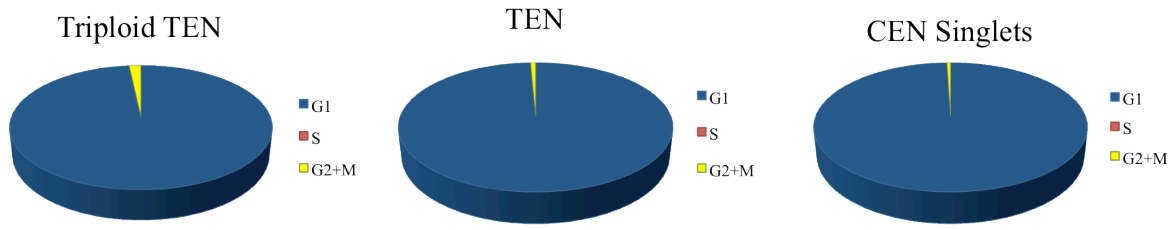

Fig 1. Fluorescent activated cell sorting of the CEN, TEN and Triploid TEN.

Since the DNA content of the control standards can vary depending on the reproductive stage, fluorescent activated cell sorting (FACS) was done using propidium iodide (P.I) stain. Using this flow cytometry technique, the distribution of mitotic stages can be determined in a cell. As shown in Figure 1, 99.5% of the CEN, 99.3% of the TEN and 98.3% of the Triploid TEN were in G_1 phase or the resting phase.

2.2 SAMPLE PREPARATION

We prepared the acidic thionin stain in our laboratory using a protocol from a previously published study[17]. 13.3 mL of acetic acid is mixed with 24 gm of tris® base and added with 650 ml of water until the reagents are dissolved with constant stirring. Methanol was then added to make the final volume of 1000 ml. Thereafter, 10 gm of thionin acetate (Sigma Aldrich, USA) was added followed by continuous stirring for an hour. The solution was then filtered through Gelman filter and a final thionin stain of pH 6.8 was achieved.

All nuclei were initially fixed in 50% ethanol, after which they were stained using the suspension technique. In this technique, we took 400 uL of the sample, and centrifuged it at 500g for 5 minutes. We aspirated out the supernatant, leaving behind the sample. To this we added 200 uL of thionin stain and waited for 25 minutes before it was centrifuged at 500 g for 5 minutes; hence the total staining time was 30 minutes. Similarly for 15 minutes of staining we waited for 10 minutes followed by 5 minutes of centrifugation. After that we washed it with gradations of ethanol (50%-100%) and later with xylene twice before inserting it into a syringe with optical gel (Nye SmartGel OC431A-LVP), necessary for OPTM.

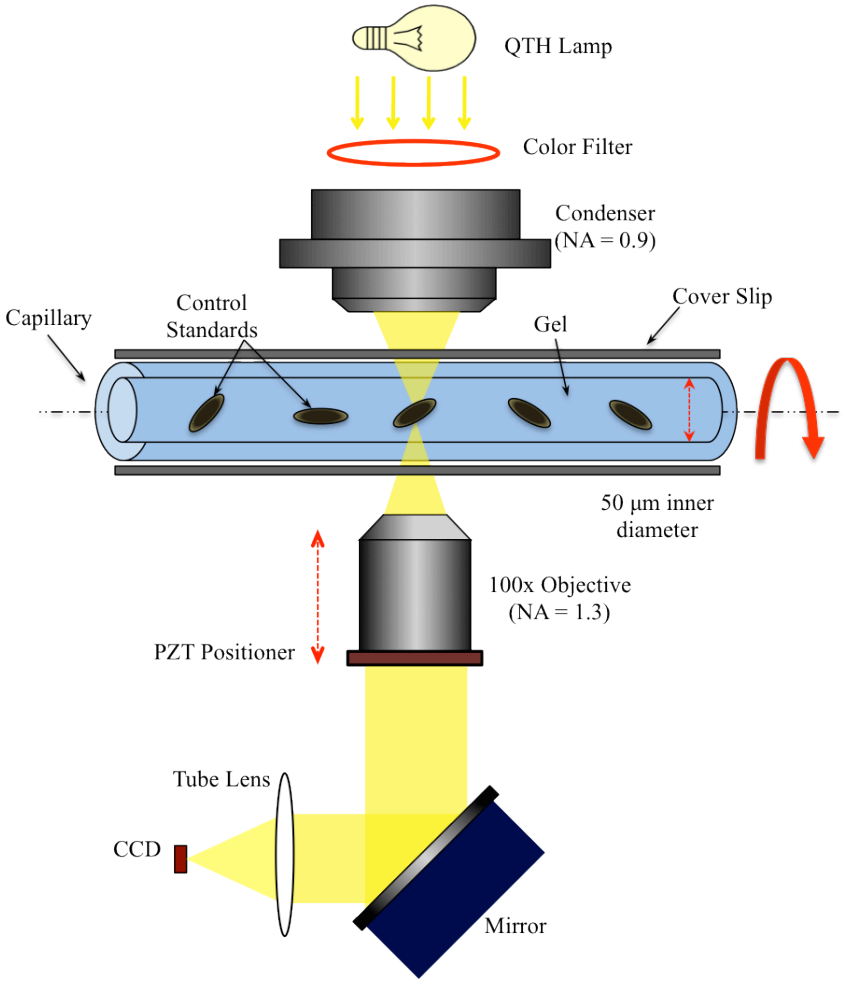

Fig 2. Schematic Diagram of an Optical Projection Tomography Microscope.

2.3 IMAGE ACQUISITION

Fifty nuclei of the three standards stained for 15 and 30 minutes were imaged using the OPTM as shown in Figure 2. The OPTM comprises of a halogen lamp (QTH) followed by a color filter having maximum transmission at

589 nm, which is the same as absorption peak of thionin stain. The sample is flowed through a capillary whose refractive index is the same as the gel in which the nuclei are suspended. The projection images are taken by a 100x objective mounted on a piezo positioner [4,5,12] focused to a CCD camera. 3D images of bare nuclei samples were acquired using the OPTM co-developed by Vision Gate Inc. (Phoenix, AZ). The OPTM generates 3D optical images by acquiring 500 2D transmission images called as pseudo-projections while the cell is being rotated at an angle division of 0.72 degrees. Similar to X-ray CT, these projection images from 360-degrees perspectives, allows the reconstruction of 3D images using the filtered back projection method. The OPTM produces 3D images of isometric resolution at 0.35 microns in various modes, such as absorption, epi-fluorescence, and epi-polarization-scattering[18].

2.4 IMAGE ANALYSIS

The reconstructed 3D images of stained bare nuclei are 16 bit and their negatives are sent to Cornell University (Ithaca, NY) for 3D segmentation. Image segmentation for the nucleus and any residual cytoplasmic regions of these standards in 3D optical microscope images is based on the observation that three primary regions (background, residual cytoplasm and nucleus) have significantly different image intensities. Hence the nucleus has the highest image intensity followed by the residual cytoplasm, if it is present.

We have developed a cell segmentation method based on two observations. Firstly, manual markings are very well matched to an image threshold (as is the case for x-ray based CT images as the reconstruction image intensity is directly related to the optical density). Secondly, there is a high image gradient in most of the transition region between two different primary regions; however the gradient is not uniform along the border of the targeted region so it cannot be used as the only information for region segmentation. From empirical tests we found that the maximum in the gradient of the gradient is best correlated with the manual markings of boundary of different region types.

For the thionin stained nuclei, the first such transition occurs at the surface of the nuclear envelope, since there is no cytoplasm, however sometimes residual cytoplasmic regions are seen. For an optical-tomography 3D image I, with a central image slice I_c, the following were the steps used for 3D segmentation of the nuclei from the background:

1. Edge enhancement was carried out using an algorithm from Deriche[19,20]. The gradient magnitude of the central slice image I_c was calculated. Further, its gradient magnitude was computed and termed as g_c.

$$g_C = \left\| \nabla \| \nabla (I_C) \| \right\|$$

2. A merit mapping of I_c was generated, where for every possible image intensity i, a merit value (m_i) was computed. For this, the boundary (B_i) of the binary region selected by that image intensity was computed. After which, the mean value of the gradient image (calculated in step 1) over the pixels belonging to the region boundary was calculated and termed as merit value:

$$m_i = \sum_{B_i} g_c / \| B_i \|$$

3. The peaks in the merit map serve as the threshold to segment the three primary regions. Typically for a cell, the threshold that corresponds to the first peak (maximum value) of the merit mapping (i.e. the mean gradient) is selected as the segmentation threshold for the cytoplasm and the threshold that corresponds to the second peak is selected as the segmentation threshold for the nucleus. But since these thionin stained nuclei have no cytoplasm, only the first peak was considered to compute the full 3D segmentation of the nuclear region.

For example, for a Triploid TEN 3D image, Figure 3a shows the histogram of the central slice of the nuclei image, while Figure 3b shows the merit function across the same range of intensity values. Both the graphs are scaled down from 16 bit to 8 bit for better understanding. The threshold was identified by the location of the first peak in Figure 3b which was at intensity *i*=94. However there was no visible feature in the histogram relating to that value. In this example there were two significant peaks in m_i, only the first peak was used as an estimate to compute the threshold for the nuclear membrane. The second peak corresponds to features within the nucleus. The central slice

image I_c is shown in Figure 4a and the automatically detected region boundary is shown in Figure 4b. In Figure 5, a surface rendering of the whole segmented nucleus is shown for three orthogonal viewing directions. Figure 5a is viewed from the same direction as Figure 4. The triploid TEN had a very eccentric profile, which was not well seen with only the central slice image. A second segmented image example is shown in Figures 6 and 7 for comparison with Triploid TEN. This case is for a CEN, which was more spherical and had an eccentricity close to 1.

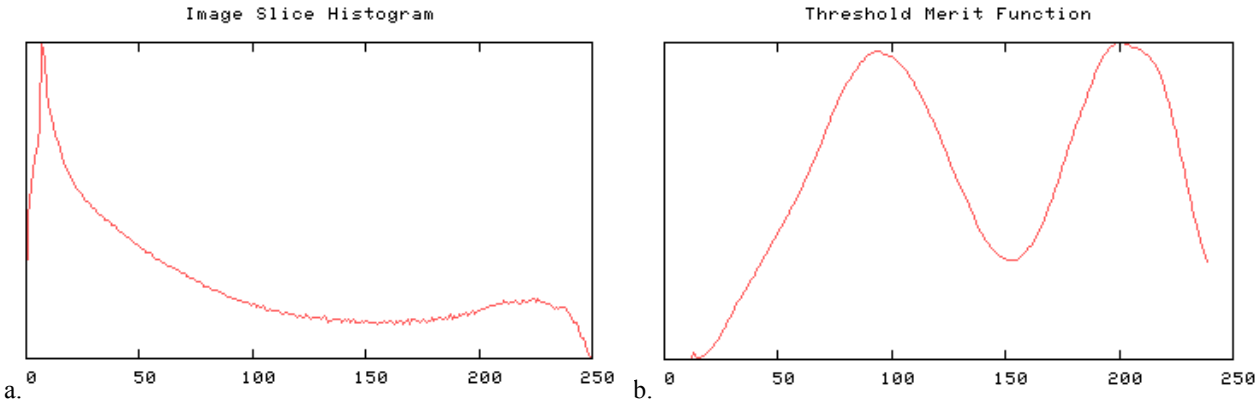

a. b.

Fig 3. a. Histogram b. Merit function (m_i) of the central slice (I_c) of a Triploid TEN nucleus image.

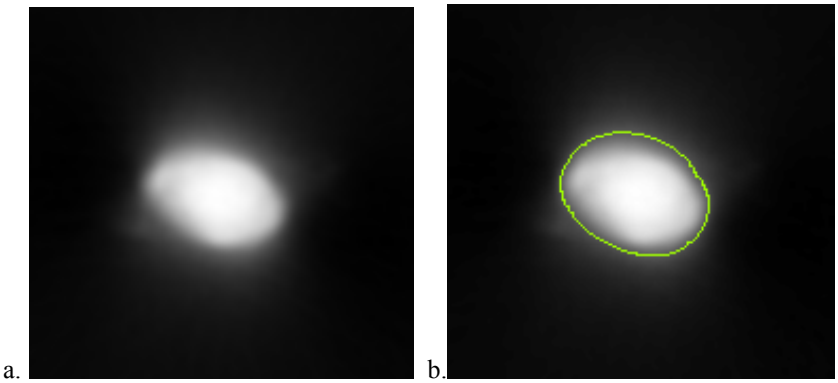
a. b.

Fig 4. a. The central slice of Triploid TEN nucleus image; b. The computed region boundary superimposed to it.

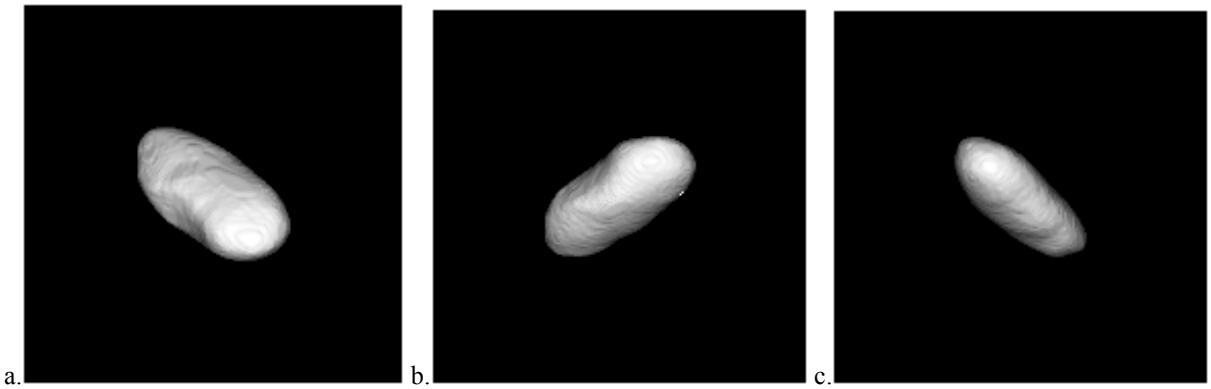
a. b. c.

Fig 5. 3D renderings of the orthogonal view of the final Triploid TEN nuclear region computed by applying the automatically determined threshold to the whole 3D image (a. axial view; b. coronal view; c. sagittal view)

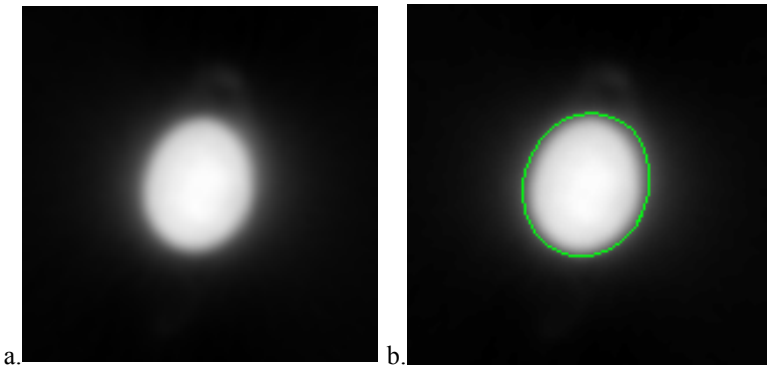

Fig 6. a. The central slice of a CEN nucleus image; b. The computed region boundary superimposed to it.

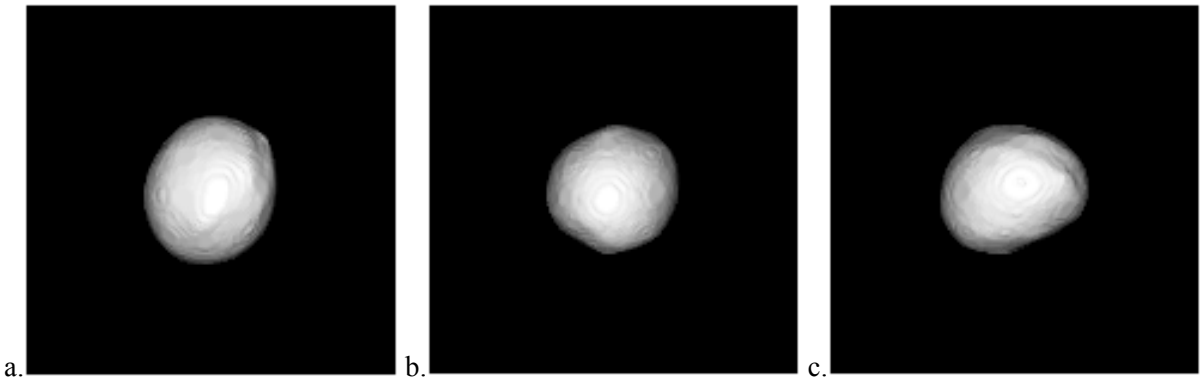

Fig 7. 3D renderings of the orthogonal views of a CEN nucleus (a. axial view; b. coronal view; c. sagittal view)

Using the above segmentation algorithm with implementation in the VisionX/SIMBA environment[21], 3D segmentation of CEN, TEN and Triploid TEN was achieved as shown in Figure 8 and 9. Camera sensor was assumed to be linear. Uniform illumination was maintained by adjusting the focus and the position of the condenser. For each cell, intensities of all the pixels in the segmented slices were added to obtain the total intensity of the 3D nucleus. Since thionin is DNA specific, the total intensity of the 3D nucleus will be proportional to the amount of DNA content in that nucleus. Ratios of the total intensities between all the three nuclei were generated for both the time periods. They were compared with the ratio of the DNA indices of the three flow cytometry standards, which are 1.5 for Triploid TEN/TEN, 3.42 for Triploid TEN/CEN and 2.28 for TEN/CEN. For each ratio, the mean and the standard deviation of the ratio of individual observations were computed using STATA 12.

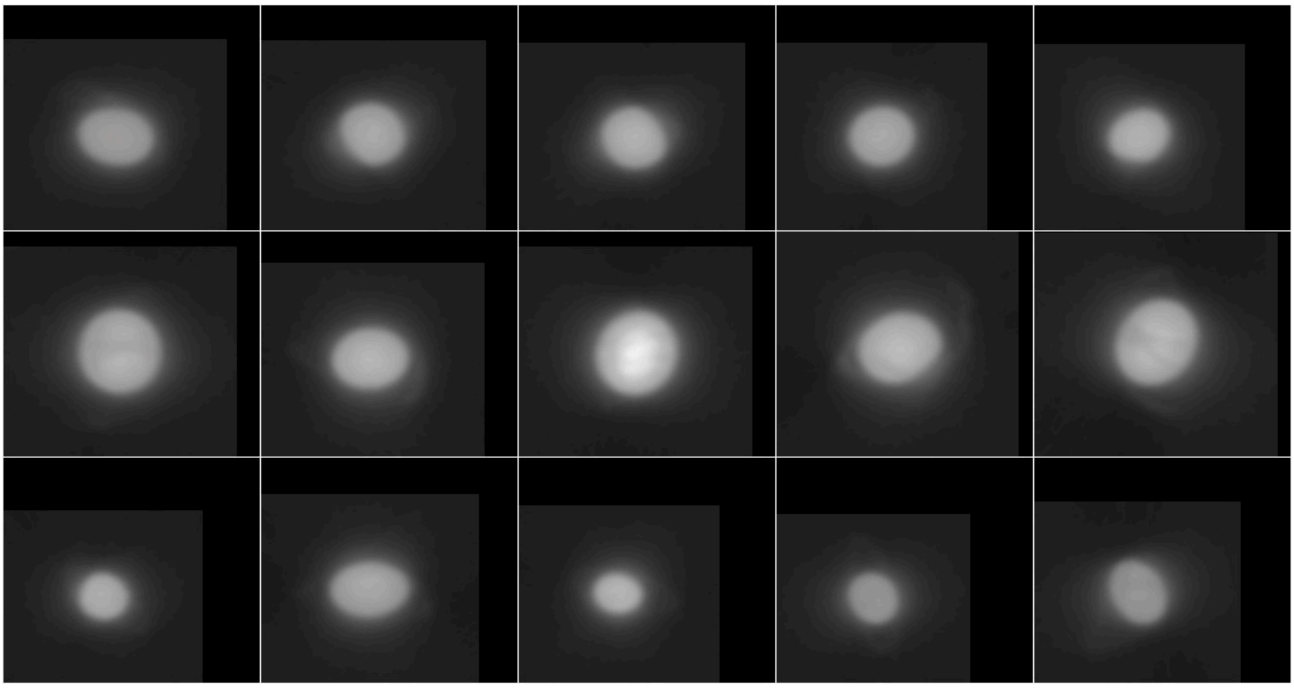

Fig 8. Centrally selected image slices from the 3D image data of the nuclei: the first top row is TEN, the second row is Triploid TEN and the third bottom row is CEN with 30 mins of staining time.

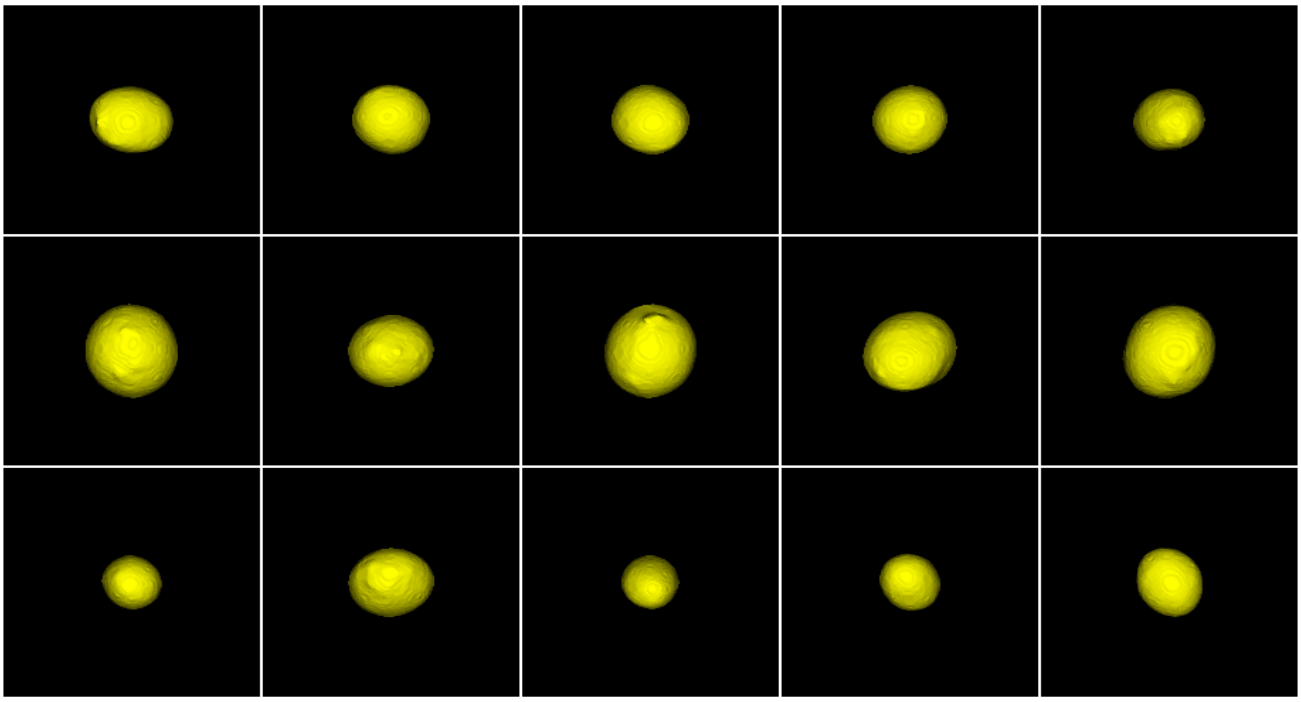

Fig 9. 3D Visualization of the segmented nuclei images. The nucleus is solid yellow: the first top row is TEN, the second row is Triploid TEN and the third bottom row is CEN with 30 mins of staining time.

3. RESULTS

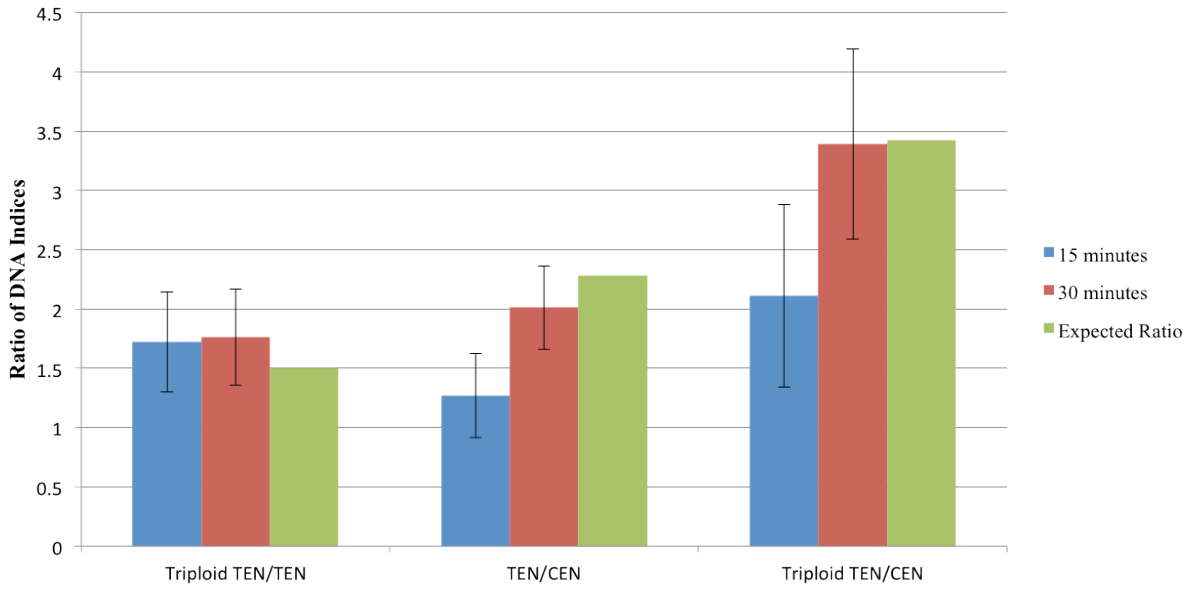

Fig 10. Mean and standard deviation of ratios of individual observations along with the expected ratios of the DNA indices of Triploid TEN, TEN and CEN at 15 and 30 minutes of thionin staining.

Fifty nuclei of all three types of cells were stained with acidic thionin and imaged using the OPTM. Figure 10 shows the expected and the measured ratios of DNA indices of Triploid TEN, TEN and CEN at 15 and 30 minutes of thionin staining along with their standard deviations. At 15 minutes, the ratio of Triploid TEN to TEN was 1.72, TEN to CEN was 1.27 and Triploid TEN to CEN was 2.11 respectively. At 30 minutes, the ratio of Triploid TEN to TEN was 1.76, TEN to CEN was 2.01 and Triploid TEN to CEN was 3.395 respectively.

The mean of the absolute deviation (mean error) between the ratio of each individual observations and the expected ratio was computed for both the staining times. Estimates of ratios of DNA indices for all three types of nuclei had less mean error at 30 minutes of staining; Triploid TEN to TEN 0.349±0.04 (97%CI 0.246-0.453), TEN to CEN 0.36±0.04 (97%CI 0.267-0.447) and Triploid TEN to CEN 0.64 ± 0.07 (97%CI 0.485-0.804). The same at 15 minutes between Triploid TEN to TEN was 0.352±0.05 (97%CI 0.23-0.47), TEN to CEN 1.004±0.07 (97%CI 0.83-1.17) and Triploid TEN to CEN 1.36 ± 0.13 (97%CI 1.05-1.67).

4. DISCUSSION & CONCLUSION

Cancer is one of leading causes of mortality in the world with late diagnosis a leading contributor. Hence early diagnosis can have a significant impact on reducing cancer related mortality. Scientists are continuously searching for newer biomarkers, which can differentiate a normal cell from a cancer cell. One such established biomarker is abnormally high nuclear chromatin content. Assessment of nuclear chromatin content requires two steps: an initial staining of the cell followed by 3D imaging of this stained cell. In the present study, we have tried to improve not only quantitative chromatin staining but also measurement of nuclear volume from 3D images. This in the future is likely to be an important tool to distinguish a cancer cell from normal one.

We took three cell standards, CEN, TEN and Triploid TEN as internal standards, which are likely to increase the reliability of the procedure as compared to two standards usually taken by previous studies[22,23,24]. The three standards were stained by thionin for two time periods in order to find the optimal staining time. The mean error was much smaller for 30 minutes as compared to 15 minutes of thionin staining except for the ratio of Triploid TEN/TEN where it was almost the same. This could be possibly because the DNA content in both of them is roughly the same, while in the other two ratios the nuclei have a large difference in DNA content. The mean error of Triploid TEN/CEN

was slightly more than the other two ratios for 30 minutes of staining due to the fact that its standard deviation as seen in Figure 10 was the highest as compared to rest of the two ratios.

Another possible factor, which could account for the variation in the mean error, is the fact these nuclei could be dividing at the time when they were being fixed in ethanol[25]. Hence a FACS scan was done for these nuclei before fixing. As shown in Figure 1, most of the nuclei of the three flow cytometer standards were in G_1 phase, which is the resting phase. However 1-2% of them were in G_2+M phase, which is the dividing phase making their DNA content highly unpredictable.

The mean error was the highest in the ratio of intensities of Triploid TEN /CEN and TEN/CEN, possibly because the DNA content of chicken erythrocytes varies with sex. Male tend to have higher DNA content as compared to female chickens[26]. However both male and female trout erythrocytes almost have the same size of sex chromosomes and hence the DNA variations due to sex related changes could be ignored for them[22]. And since we had used mixed populations of both chicken and trout erythrocytes the standard deviation and hence the mean error is seen maximum when CEN is present in the ratio.

Currently ACIS uses feulgen staining technique and 2D image cytometry, which is time consuming and destroys the morphology, one of the very important features[27,28] used in conventional cytology for early cancer diagnosis. Dai *et. al* used a DNA index of 1.1 to get a sensitivity and specificity of 100% and 14.3% respectively for pancreatic cancer[29]. From the consensus report of ESCAP a cell is considered aneuploidy if its DNA content deviates more than 10% (DNA index of 1.1) from the diploid cell[30,31]. Alanen *et. al* used a DNA index of 1.2 to get a sensitivity and specificity of 82% and 33% respectively for breast cancer[32]. Faranda *et. al* used a DNA index of 1.25 and got an sensitivity of 79%, 68%, 88%, 52%, 61% for oral, cervix, bladder, colorectal and breast cancer respectively[33].

We used thionin stain with 3D imaging using OPTM, which preserves morphology. 30 minutes of staining on an average showed more stociometricity than 15 minutes. Considering the mean error of Triploid TEN/TEN at 30 minutes as the other two have more variability, a DNA index of 1.35 (35% mean error) will successfully be able to distinguish a malignant cell from a normal cell. To reduce the mean error to 10%, a thionin staining of 45 minutes could be performed. Since thionin doesn't overstain, more staining time will make it even more stoichiometric than 15 and 30 minutes. Another method to reduce the mean error is to improve the 3D segmentation technique on the 3D reconstructed images. Since these standards are bare nuclei, which are processed from full erythrocytes, some amount of cytoplasm will always be present. This is likely to cause errors in 3D segmentation of the images.

Hence to conclude, with the current technique we can distinguish a cancer cell only if its DNA index is equal to or more than 1.35. Further improvements have to be made in order to identify cancer cells with a DNA index as close as 1.1 to normal human diploid cell.

5. NEW OR BREAKTHROUGH WORK PRESENTED

In this paper we present a novel technique for quantitative measurement using OPTM. Also to our knowledge, we are the first to successfully perform 3D segmentation of nucleus to measure its chromatin content by using absorption stain.

ACKNOWLEDGEMENTS

Technical support and training were gratefully provided by time spent with Sarah Shimer, Ben Hawthorne, Ryland Bryant, Mathew Watson, Christy Lancaster, David Steinhauer, and Jon Hayenga of VisionGate Inc., R&D center in Seattle. Funding for this Interdisciplinary and Collaborative NSF project was provided by National Science Foundation, grant # CBET-1014976 (PI's are E.J. Seibel & A.P. Reeves).

REFERENCES

[1]. Gill, J.E., Wheeless, L.L., Madden. C.H., Marisa. R.J., Horan, P.K., "A comparison of acridine orange and Feulgen cytochemistry of human tumor cell nuclei," Cancer Res. 38(7), 1893-8 (1978).

[2]. Lazcano, O., Chen, L., Tsai. C., Li, C.Y., Katzmann, J., Sebo, T., Kimlinger, T., Baker, J., "Image Analysis and Flow Cytometric DNA Studies of Benign and Malignant Body Cavity Fluids: Reappraisal of the Role of Current Methods in the Differential Diagnosis of Reactive Versus Malignant Conditions," Mod Pathol. 13(7), 788–796, (2000).

[3]. Sherman, A.B., Koss, L.G., Wyschogrod, D., Melder, K.H., Eppich, E.M., Bales, C.E., "Bladder cancer diagnosis by computer image analysis of cells in the sediment of voided urine using a video scanning system," Anal Quant Cytol Histol. 8(3), 177-86, (1986).

[4]. Fauver, M., Seibel, E.J., Rahn, J.R., Meyer, M.G., Patten, F.W., Neumann, T., Nelson, A.C., "Three-dimensional imaging of single isolated cell nuclei using optical projection tomography," Opt. Express 13:4210, (2005).

[5]. Meyer, M.G., Fauver, M., Rahn, J. R., Neumann, T., Patten, F.W., Seibel, E.J., Nelson, A.C., "Automated cell analysis in 2D and 3D: A comparative study," Patt. Recog. 41, 141-146 (2009).

[6]. Levy, M., Oberg, T., Campion, M., Clayton, A., Halling, K., Henry, M., Kipp, B., Sebo, T., Zhang, J., Enders, F., Clain, J., Gleeson, F., Rajan, E., Roberts, L., Topazian, M., Wang, K., Gores, G., "Comparison of Methods to Detect Neoplasia in Patients Undergoing Endoscopic Ultrasound-Guided Fine-Needle Aspiration," Gastroenterology 142:1112–1121 (2012).

[7]. Schulte, E., Wittekind, D., "Standardization of the Papanicolaou stain. I.A comparison of five nuclear stains," Analytical Quantitative Cytology Histology Jun 12(3) 149-56 (1990).

[8]. Schulte, E.K., Fink, D.K., "Hematoxylin staining in quantitative DNA cytometry: an image analysis study," Analytical Cellular Pathology 9(4) 257–268 (1995).

[9]. Schulte, E., Wittekind, D., "Standardization thionin-eosin stain in bronchial cytology. A substitute for haematoxylin-eosin Y staining," Analytical Quantitative Cytology Histology 11(2) 131-9 (1989).

[10]. Swartza, R., West, L., Boiko, I., Malpica, A., Guillaud, M., MacAulay, C., Follen, M., Atkinson, E.N., Cox, D.D., "Classification using the cumulative log-odds in the quantitative pathologic diagnosis of adenocarcinoma of the cervix," Gynecologic Oncology S24 – S31 (2005).

[11]. Chieco, P., Derenzini, M., "The Feulgen reaction 75 years on", Histochem & Cell Biology 111(5), 345–358 (1999).

[12]. Faranda, A., Costa, A., Canova, S., Abolafio, G., Silvestrini, R., "Image and flow cytometric analyses of DNA content in human solid tumors. A comparative study," Anal and Quan Cytology and Hist., 19(4), 338–344, (1997).

[13]. Schmidt, D., Wischmeyer, P., Leuschner, I., Sprenger, E., Langenau, E., Schweinitz, D. V., Harms, D., "DNA analysis in hepatoblastoma by flow and image cytometry," Cancer 72(10) 2914–2919 (1993).

[14]. Huang, Q., Yu, C., Klein, M., Fang, J., Goyal, R.K., "DNA index determination with Automated Cellular Imaging System (ACIS) in Barrett's esophagus: comparison with CAS 200," BMC Clinical Pathology 5: 7 (2005)

[15]. Rendon, A.T., Stewart, R., Craig, G.T., Wells, M., Speight, P.M., "DNA ploidy analysis by image cytometry helps to identify oral epithelial dysplasias with a high risk of malignant progression," Oral Oncology 45(6), 468–473 (2009).

[16]. Huang, Q., Yu, C., Klein, M., Fang, J., Goyal, R.K., "DNA index determination with Automated Cellular Imaging System (ACIS) in Barrett's esophagus: comparison with CAS 200," BMC Clinical Pathology 5 7 (2005).

[17]. Zahniser, D.J., Lapen, D.C., Oud, P.S., "Thionin staining and imaging technique," US patent number: 5168066, issue date Dec 1 (1992).

[18]. Miao, Q., Reeves, A., Patten, F.W., Seibel, E.J., "Multimodal 3D Imaging of Cells and Tissue, Bridging the Gap Between Clinical and Research Microscopy," Ann of Biomed Eng. 40(2) 263-76 (2012).

[19]. Deriche, R., "Using Canny's Criteria to Derive a Recursively Implemented Optimal Edge Detector," International Journal of Computer Vision 1(2) 167-187, (1987).

[20]. Monga, O., Deriche, R., Rocchisani, J.M., "3D edge detection using recursive filtering: Application to scanner images," CVGIP: Image Understanding 53 76–87, (1991).

[21]. Reeves, A.P., "Cornell university vision and image analysis group," http://www.via.cornell.edu/visionx/.

[22]. Vindeløv, L.L., Christensen, I.J., Nissen, N.I., "Standardization of high-resolution flow cytometric DNA analysis by the simultaneous use of chicken and trout red blood cells as internal reference standards," Cytometry 3(5) 328-31, (1983).

[23]. Espinosa, E., Josa, A., Gil, L., Martí, J.I., "Triploidy in rainbow trout determined by computer-assisted analysis," Journal of Exp. Zoology 303 1007–1012, (2005).

[24]. Pierrez, J., Ronot, X., "Use of diploid and triploid trout erythrocytes as internal standards in flow cytometry," Cytometry 12 275-278, (1991).

[25]. Vindeløv, L., Christensen, J., Jensen, G., Nissen, N., "Limits of detection of nuclear DNA abnormalities by flow cytometric DNA analysis. Results obtained by a set of methods for sample-storage, staining and internal standardization," Cytometry Mar 3(5) 332-9, (1983).

[26]. Mendonça, M.A., Carvalho, C.R., Clarindo, W.R., "DNA Content Differences Between Male and Female Chicken Nuclei and Z and W Chromosomes Resolved by Image Cytometry," J Histochem Cytochem. 58(3) 229-35, (2010).

[27]. Koestner, A., "Prognostic Role of Cell Morphology of Animal Tumors," Toxicologic Pathology 13(2) 90–94, (1985).

[28]. Wolberg, W. H., Street, W. N., Mangasarian, O. L., "Importance of nuclear morphology in breast cancer prognosis," Clinical Cancer Research 5(11) 3542–3548, (1999).

[29]. Dai, S.C., Weinberg, A., Rajendran, L., Nigam, S., Sharma, A., Kirtane, T., "Automated Cellular Imaging System for Aneuploidy Differentiates Chronic Pancreatitis From Pancreatic Cancer," Gastroenterology 142(5) S–849–849, (2012)

[30]. Böcking, A., Giroud, F., Reith, A., "Consensus report of the ESACP task force on standardization of diagnostic DNA image cytometry," Analytical cellular pathology 8 67–74, (1995).

[31]. Haroske, G., Baak, J.P., Danielsen, H., Giroud, F., Gschwendtner, A., Oberholzer, M., "Fourth updated ESACP consensus report on diagnostic DNA image cytometry", Analytical cellular pathology 23 89–95, (2001).

[32]. Alanen, K.A., Lintu, M., Joensuu, H., "Image cytometry of breast carcinomas that are DNA diploid by flow cytometry: time to revise the concept of DNA diploidy?," Anal Quant Cytol Histol 20 178-186, (1998).

[33]. Faranda, A., Costa, A., Canova, S., Abolafio, G., Silvestrini, R., "Image and flow cytometric analyses of DNA content in human solid tumors. A comparative study," Anal and Quan Cytology and Hist. 19(4), 338–344, (1997).